REPORT DOCUMENTATION PAGE

Form Approved
OMB No. 0704-0188

1. REPORT DATE *(DD-MM-YYYY)*	2. REPORT TYPE	3. DATES COVERED *(From - To)*
19-02-2013	Journal Article	October 2012-February 2013

4. TITLE AND SUBTITLE

Photoinduced partial unfolding of tubulin bound to meso- tetrakis (sulfonatophenyl) porphyrin leads to inhibition of microtubule formation *in vitro*

5a. CONTRACT NUMBER
FA8650-08-6930

5b. GRANT NUMBER

5c. PROGRAM ELEMENT NUMBER
0602202F

6. AUTHOR(S)
Brady McMicken, Robert J. Thomas, Lorenzo Brancaleon

5d. PROJECT NUMBER
7757

5e. TASK NUMBER
HD

5f. WORK UNIT NUMBER
04

7. PERFORMING ORGANIZATION NAME(S) AND ADDRESS(ES)
Air Force Research Laboratory
711th Human Performance Wing
Human Effectiveness Directorate
Bioeffets Division
Optical Radiation Bioeffects Branch
4141 Petroleum Rd Bldg 3260
JBSA Fort Sam Houston, Texas 78234

8. PERFORMING ORGANIZATION REPORT NUMBER

9. SPONSORING / MONITORING AGENCY NAME(S) AND ADDRESS(ES)
Air Force Research Laboratory
711th Human Performance Wing
Human Effectiveness Directorate
Bioeffets Division
Optical Radiation and Bioeffects Branch
4141 Petroleum Rd Bldg 3260
JBSA Fort Sam Houston, Texas 78234

TASC, Inc.
4141 Petroleum Rd
JBSA Fort Sam Houston, Texas 78234

10. SPONSOR/MONITOR'S ACRONYM(S)
711 HPW/RHDO

11. SPONSOR/MONITOR'S REPORT NUMBER(S)
AFRL-RH-FS-JA-2013-0008

12. DISTRIBUTION / AVAILABILITY STATEMENT
Distribution A: Approved for public release; distribution unlimited (approval given by local Public Affairs Office TSRL-PA-13-0077)

13. SUPPLEMENTARY NOTES

14. ABSTRACT

We investigated the effects of irradiating the complex formed by meso-tetrakis (sulfonatophenyl) porphyrin (TSPP) and tubulin in an attempt to induce unfolding of tubulin through the mediated photophysics of the porphyrin. Tubulin is an important protein which forms microtubules and has been a target of anticancer treatments. We used a combination of spectroscopic techniques to gain insight into the structural changes induced by the photosensitizer on the protein. In air-saturated samples, absorption and fluorescence spectroscopy show substantial bleaching of the porphyrin upon laser irradiation. The bleaching is accompanied by a sharp decrease (~ 2 ns) in the average decay lifetime of the protein and a spectra shift of the dichroic spectrum consistent with a decrease of helical structure and an increase in the relative contribution of β-structure and random coil. The effect of deoxygenation of the sample (using the freeze-thaw method or the N_2 purging) was also considered and the results were interpreted in the context of similar proteins. The results indicate that there is indeed significant unfolding of tubulin as a result of irradiating the bound porphyrin. Atomic force microscopy (AFM) shows that the photoinduced conformational changes inhibit the formation of microtubules *in vitro*.

15. SUBJECT TERMS

16. SECURITY CLASSIFICATION OF:			17. LIMITATION OF ABSTRACT	18. NUMBER OF PAGES	19a. NAME OF RESPONSIBLE PERSON
UNCLASSIFIED					Jeffrey Oliver, Ph.D.
a. REPORT	b. ABSTRACT	c. THIS PAGE	SAR	21	19b. TELEPHONE NUMBER *(include area code)*
U	U	U			NA

Standard Form 298 (Rev. 8-98)
Prescribed by ANSI Std. 239.18

WILEY ONLINE LIBRARY
Early View publication on
www.wileyonlinelibrary.com
(issue and page numbers not yet assigned;
citable using Digital Object Identifier – **DOI**)

J. Biophotonics 1–15 (2013) / **DOI** 10.1002/jbio.201300066

Journal of
BIOPHOTONICS

FULL ARTICLE

Photoinduced partial unfolding of tubulin bound to meso-tetrakis(sulfonatophenyl) porphyrin leads to inhibition of microtubule formation *in vitro*

Brady McMicken[1,2], *Robert J. Thomas*[2], *and Lorenzo Brancaleon*[*,1]

[1] The University of Texas at San Antonio, Department of Physics and Astronomy, One UTSA Circle, San Antonio, Texas, 78249 USA
[2] Optical Radiation Bioeffects Branch, Bioeffects Division, Air Force Research Laboratory, Fort Sam Houston, Texas 78234, USA

Received 1 May 2013, revised 4 June 2013, accepted 19 June 2013
Published online 30 July 2013

Key words: tubulin, porphyrin, circular dichroism, protein unfolding, atomic force microscopy

Supporting information for this article is available free of charge under http://dx.doi.org/10.1002/jbio.201300066

The irradiation of the complex formed by meso-tetrakis (sulfonatophenyl) porphyrin (TSPP) and tubulin was investigated as well as its effects on the structure and function of the protein. We have used tubulin as a model target to investigate whether photoactive ligands docked to the protein can affect the structure and function of the protein upon exposure to visible light. We observed that laser irradiation prompts bleaching of the porphyrin which is accompanied by a sharp decrease (~2 ns) in the average fluorescence lifetime of the protein and a change in the dichroic spectrum consistent with a decrease of helical structure. The result indicated the photoinduced partial unfolding of tubulin. We also observed that such partial conformational change inhibits the formation of microtubules *in vitro*. We investigated whether photosensitization of reactive oxygen species was responsible for these effects. Even upon removal of O_2 the protein still undergoes conformational changes indicating that irradiation of the bound porphyrin does not require the presence of O_2 to prompt conformational and functional effects opening the possibility that other mechanisms (e.g., charge transfer) are responsible for the photoinduced mechanism.

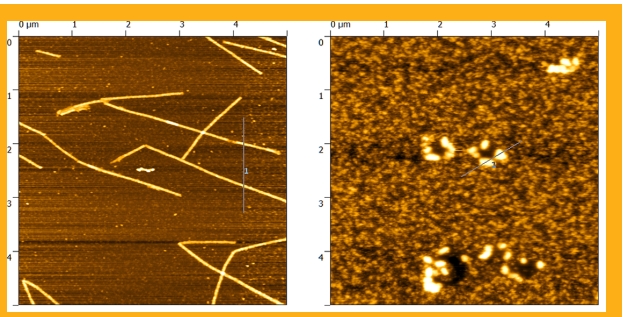

AFM images of microtubules before and after irradiation of the tubulin/TSSP complex which show how irradiation of the ligand prevents the formation of organized microtubules.

1. Introduction

The function of a protein is generally related to its structure [1] (e.g., the three-dimensional arrangement of the amino acid residues) and physical elements such as charge distribution, van der Waals interactions and the hydrogen-bond network of the folded protein. Biophysical research has investigated protein structure and its effect on protein function for many decades [2] and the ability to modify the conformation of a protein by locally changing its structure is of considerable interest for many ap-

* Corresponding author: e-mail: lorenzo.brancaleon@utsa.edu, Phone: 210-458-5694, Fax: 210-458-4919

plications because of the correlation between the structural integrity of a protein and its function. One novel method of locally unfolding a protein involves the use of a light activated ligand which triggers photophysical events capable of prompting conformational changes in the polypeptide. Such approach can be used to prompt a localized conformational modification that maintains the substantial structural integrity of the protein rather than producing massive unfolding. Photoisomerization [3, 4] as well as photosensitization of singlet oxygen [5, 6] have been suggested as mechanisms to prompt conformational changes in peptides and proteins. Our group has demonstrated that irradiation of ligands can alter the structure of proteins with mechanisms that do not depend on isomerization or oxygen sensitization [7, 8]. What was the initial biomedical investigation, has now morphed into a more basic biophysical approach to address the questions raised by the effects of laser irradiation on proteins. For instance, using a combination of Resonance Raman Spectroscopy (RRS), density functional theory (DFT) and docking simulations we have started to address the problem of establishing the location of the ligand [9]. We demonstrated that the approach is promising by establishing that certain porphyrins are able to prompt conformational changes in small globular proteins [7, 8]. In this study, we have adopted a different protein model (tubulin) and investigated the effects of the irradiation of a water-soluble porphyirn ligand (meso-tetrakis (sulfonatophenyl)porphyrin, TSPP) on the structure of the protein. Compared to previous models tubulin offers the opportunity to test the functional effects of the photoinduced structural changes by following the formation of microtubules (MTs) *in vitro* [10, 11].

Tubulin is a ubiquitous, 55 kDa globular protein which natively appears in several, structurally similar variants (i.e. α, β, γ) [12]. The most abundant variants, α and β, assemble into heterodimers that form the basic building block of microtubules (MT) [10, 11]. The formation of MT *in vivo* is mediated by additional factors such as the hydrolization of guanosine-5-triphophate (GTP) at the leading edge of the MT [13, 14]. MT are key to a number of important functions such as intracellular transport, morphogenesis, mitosis and meiosis [15, 16]. Because tubulin heterodimers and MTs are vital for cellular processes, they have become a prime target in biomedical research [17–19].

Besides the basic biophysical challenge of relating the photoinduced conformational changes with functional modification of the protein, the potential for the photoinduced disruption of MT is another motivation for the work presented here, as this could be exploited for novel approaches in biomedical applications such as phototherapy. In fact, direct photoinduced conformational changes of proteins could offer an alternative to the current paradigm for photodynamic therapy (PDT) which is based on the diffusion-limited photosensitization of cytotoxic singlet oxygen and other reactive oxygen species (ROS) [20–23]. Porphyrins are often used in phototherapy because of their large quantum yields for the formation of triplet states [24], however the possibility of using them to selectively modify protein functions can offer a new approach in their use especially if one can demonstrate a path of photosensitization that does not depend on diffusing O_2.

From both the biophysical and biomedical standpoint the dependence on a diffusion mechanism brings limitations. Therefore, the emphasis in our research is the investigation of localized photoinduced mechanisms that target proteins at a specific location (e.g., where the photoactive ligand is docked) and cause local (or partial) but significant conformational changes that can potentially modify the function of a protein without necessarily change its structural integrity. We have demonstrated that localized changes can be prompted by porphyrins [7, 8]. In this investigation we have changed the focus from showing the ability to photoinduced localized conformational changes to relating these changes to functional modifications. We selected tubulin as the protein model because is a more biomedically relevant protein than the model we used previously and one of its functions (e.g., the ability to self-assemble into MT) is relatively easy to test. We showed that TSPP binds tubulin between the taxol and the GTP/GDP sites with an affinity of $\sim 1.1 \times 10^6\ M^{-1}$, and that the binding does not interfere with the ability to form MT [25] so that any influence on tubulin self-assembly can be attributed to photoinduced effects. In addition, Guo et al. showed that irradiation of rhodamine-tags triggers depolymerization of MT upon laser exposure [26], thus indicating that visible light could be used to affect the formation of MT. With the current investigation we have studied whether i.) TSPP can trigger conformational changes in tubulin upon low-intensity visible irradiation, and ii.) the conformational changes affect the ability of tubulin to assemble into MT. We also indicated possible photochemical/photophysical mechanisms responsible for the conformational changes.

2. Experimental

2.1 Sample preparation

TSPP (Frontier Scientific, Logan, UT) and tubulin from porcine brain, >99% pure, (T240, Cytoskeleton, Denver, CO) were used without further purification. All experiments were carried out at pH ~7, however

the buffer preparation was different depending on the experiment. For most spectroscopic measurements phosphate buffered saline tablets were dissolved in deionized water (Sigma-Aldrich, St. Louis, MO) to provide a 10 mM buffer at pH 7.4. However, the same buffer preparation could not be used for circular dichroism (CD) experiments due to its high optical density in the UV created by the chloride counter ions [32]. Thus, for CD experiments a 10 mM buffer at pH 7.4 was prepared using monobasic KH_2PO_4 and NaOH with NaF used to adjust the ionic strength (all chemicals were purchased from Sigma Aldrich, St.Louis, MO). The formation of MT also required a unique buffer which contains 50 mM PIPES, 2 mM $MgCl_2$, 10% glycerol, and 1 mM EGTA in deionized water. GTP (2 mM) was also added to this buffer to promote polymerization at 37 °C.

The concentrations of TSPP and tubulin were determined spectroscopically using Beer-Lambert law [27] with $\varepsilon_{280} = 1.15 \times 10^5\ M^{-1}\ cm^{-1}$ for Tubulin and $\varepsilon_{413} = 5.10 \times 10^5\ M^{-1}\ cm^{-1}$ [28] for TSPP. Specific concentrations for each type of experiments is provided below.

2.2 Absorption spectroscopy

Absorption spectroscopy was performed using a dual-beam spectrophotometer (Evolution 300, Thermo Fisher Scientific, Waltham, MA) with a 2 nm bandwidth at a 240 nm/min speed. Absorption spectra were recorded in the region between 250 nm and 460 nm in a 1 cm pathlength quartz cuvette (Starna Cells Inc., Atascadero, CA) with baseline correction.

2.3 Steady state fluorescence spectroscopy

Fluorescence spectra were recorded using a double monochromator flourometer (AB2, Thermo Fisher Scientific, Waltham, MA). All spectra were recorded with a bandpass of 4 nm in both excitation and emission with integration time of 1 s at 1 nm steps. Spectra of tubulin were collected between 300 nm and 450 nm with excitation wavelength, λ_{ex}, at 295 nm. At this wavelength the 8 Trp residues of the tubulin dimer are exclusively excited over the other aromatic amino acids [25]. Spectra of TSPP were recorded in the 580–750 nm range using $\lambda_{ex} = 413$ nm. The optical density at λ_{ex} was kept under 0.15 to ensure a uniform distribution of energy throughout the sample and avoid inner filter effects [29]. Tubulin to TSPP molar ratio was kept at 1 : 1. To obtain such a ratio the maximum of the Soret band absorption of TSPP is 4.43 times larger than the maximum of the absorption of tubulin at 280 nm.

The emission intensity was calculated by integrating the area under the emission peak of the spectrum corrected for instrument response (data file provided by the manufacturer). The emission was normalized for the absorbed radiation according to [27]

$$F_{corr} = F_{raw} 10^{\left(\frac{A_{ex}+A_{em}}{2}\right)} \quad (1)$$

where F_{raw} is raw fluorescence intensity data, A_{ex} is the optical density of the sample at the excitation wavelength and A_{em} is the optical density at the maximum emission wavelength.

2.4 Time-resolved fluorescence

Fluorescence decay of tubulin was recorded using a time-correlated single-photon-counting (TCSPC) instrument (Fluorocube, Horiba Scientific, Edison, NJ). The solution was excited with a pulsed source (~700 ps pulsewidth, 1 MHz rep. rate) at 293 nm to probe the Trp residues of the protein. The emission was recorded at 330 ± 8 nm which includes the maximum of the fluorescence of tubulin. The fluorescence decay was analyzed using the deconvolution software DAS6 (Horiba Scientific). The software uses an iterative re-convolution of the source time profile of the instrument, $G(t)$ or prompt, with the theoretical fluorescence decay modeled as a sum of exponentials.

$$F(t) = \Sigma_i A_i\, e^{-\frac{t}{\tau_i}} \quad (2)$$

where A_i is the amplitude and τ_i is the lifetime of the i-th component. $G(t)$ is recorded from a scattering sample that does not fluoresce (in this case a 1 mg/ml suspension of glycogen in water) and setting the emission monochromator at the same wavelength as the pulsed source. Both $F(t)$ and $G(t)$ are recorded at a sampling rate $< 2.5\%$ of the maximum repetition rate of the pulsed source in order to avoid non-linear effects in the acquisition [30]. The convolution of $F(t)$ and $G(t)$ is fitted, using a the least-squares method, to the experimental decay curve, $I(t)$, by iterative change of the amplitude and lifetime parameters. The quality of the fit is determined be ensuring values of χ^2 between 1 and 1.5 and values of the Durbin-Watson parameter between 1.8 and 2.0 [30]. The average lifetime of the decay can then be expressed as:

$$\langle \tau \rangle = \Sigma_i A_i \tau_i \quad (3)$$

2.5 Resonance Raman Spectroscopy (RRS)

RRS experiments were conducted using the 413 nm emission of a Kr^+ gas laser (Coherent Innova Krypton ion laser). This corresponds to the wavelength of the maximum of absorption of TSPP. The incident power at the sample was kept at 15 mW. Light scattered from the sample was collected perpendicular from the incoming excitation laser beam and then sent to a double monochromator (Spex 1404, Horiba Scientific) equipped with an Andor iDus 420A-BV back-illuminated 1024×256 pixel CCD camera (Andor, Belfast, United Kingdom). Spectra were digitized, stored and analyzed using LabSpec (Horiba Scientific). Data was collected in the region between 150 cm^{-1} and 1800 cm^{-1} where the main structural bands of TSPP can be found [31].

2.6 Circular dichroism

CD was carried out using a DSM 14 Spectropolarimeter (Olis Inc., Bogart, GA). The signal of tubulin was measured in the UV region between 185 nm and 240 nm with the solution in a 1 mm path length quartz cuvette. This is the region of the $\pi \rightarrow \pi^*$ transition band of the amide (peptide bond) and is known to produce a CD signal that is sensitive to the secondary structure of the polypeptide [32]. For CD experiments the optical density of the solution containing the TSPP/tubulin complex was kept ~0.9 at 220 nm in order to optimize the S/N ratio [33]. This corresponds approximately to a tubulin concentration of 0.2 mg/mL. The S/N is kept constant by altering the integrating time depending on the PMT voltage value. This relative composition of the secondary structure in the 185–240 nm region [34] was estimated with CDPro [35]. An exhaustive survey of 4 different basis sets (SP37, SP37A, SDP42, SMP50) and 3 fitting procedures (CDSSTR, SELCON3, CONTINLL) were tested for all samples. These results were compared to the average of experimental and calculated proportions from other studies in the literature (33% α-helix, 21% β-sheets, 45% other) [36]. Ultimately the combination of the CONTINLL procedure with the basis set SMP50 was chosen because it was most accurate in predicting the accepted secondary structure of native tubulin at the pH of our samples.

2.7 Atomic Force Microscopy (AFM)

To test whether or not the conformational change of tubulin would inhibit microtubule formation, AFM was employed. Solutions containing the tubulin/TSPP complex were prepared in the assembly buffer (see above) without GTP. This solution contained 1.5 mg/mL of tubulin and thus 13.6 μM of both tubulin and TSPP. The solution was separated into two parts: one was irradiated at 405 nm for 15 min with an irradiance of 15 mW/cm^2 while the other one was kept in the dark for the duration of the irradiation. Immediately after this, GTP was added to both solutions which were then incubated at 37 °C for 45 minutes to promote formation of MT [37, 38]. These solutions were then pelleted at $25{,}000 \times g$ for 10 min at 37 °C and 20 μM of taxol was added to stabilize any microtubules that may have formed. The solution was then incubated with 0.2% glutaraldehyde to create cross linking and help immobilize microtubules to the surface [39]. After 20 minutes of incubation, a small aliquot (~20 μl) of each solution was deposited on pre-treated mica. The substrate used for adsorption and immobilization of microtubules in the AFM study was mica modified with a layer of 3-aminopropyltriethoxysilane (AP-mica) [40]. This forms a positively charged surface around neutral pH, which is capable of immobilizing the slightly negative MT (the pI being 4.96 for α-tubulin and 4.78 for β-tubulin [41]) to enable AFM imaging [42]. The deposited solution was incubated on the substrate for 5 minutes. Subsequently the mica slides were rinsed with excess buffer and gently dried with filter paper. Contact mode AFM (FTM-AFM) under ambient conditions was carried out on a XE-Bio Scanning Probe Microscope (Park Systems, Santa Clara, CA). Commercial Si_3N_4 triangular- shaped cantilevers (Ted Pella, Redding, CA) with a spring constants of 0.27 N/m and resonant frequencies of 30 kHz were used to probe the topography of the surface. Scans were done at a rate 0.75 Hz with a scan range of 5×5 μm and a resolution of 515×512 data points.

2.8 Irradiation

Irradiation of the TSPP/tubulin complex solution was carried out using a solid state 185 mW laser at 405 nm (Power Technology inc., Alexander, AR), which excites TSPP in the Soret band [25]. The laser beam is attenuated through a series of neutral density filters and defocused using a long focal length lens to make the irradiance delivered to the sample approximately 15 mW/cm^2. This relatively low-irradiance delivery is used to ensure that any protein unfolding is not due to thermal effects from the absorbed light [43] since heat is well known to denature proteins [44]. The solutions were exposed to increasing total energy doses of 0, 4.5, 13.5 and 27 J/cm^2. Absorption, fluorescence, and fluorescence lifetime spectra were taken after each irradiation. AFM and CD were measured before and after the

last dose. Control experiments were carried out by irradiating solutions containing TSPP and tubulin separately as well as on TSPP/tubulin complex solution that did not undergo laser irradiation.

2.9 Deoxygenated samples

In order to gauge whether or not any conformational changes of tubulin are induced by the formation of reactive oxygen species, additional experiments were done after eliminating O_2 from the sample solutions. Oxygen was purged by two different methods. The first method uses flow of pure N_2 (from high pressure cylinders) through a syringe and into an airtight quartz cell with a rubber diaphragm top. The O_2 purging with nitrogen was done for 20 minutes in the dark. This method however was found to dissociate the porphyrin and tubulin as shown by the absorption spectrum of TSPP after purging (Figures S1–S4 and Tables S1 and S2 in Supporting Information).

The second deoxygenating method was the classic freeze-thaw approach which involved 5 cycles in which 2 ml of the solution containing the tubulin/TSPP complex was frozen (using a mixture of dry ice and methanol) in an air-tight flask, then subjected to vacuum ($\sim 10^{-4}$ Torr) for 15 minutes and then finally thawed slowly at room temperature. Although the freeze-thaw cycles appears to induce an irreversible conformational change of the tertiary structure of tubulin which somewhat limits its value as a control experiment for deoxygenated samples its results are still presented for comparison.

Absorption, fluorescence, fluorescence lifetime and CD were recorded before and after the samples were deoxygenated. After deoxygenation, some samples were irradiated while others were left in the dark for a period of time equivalent to the time of irradiation. During the irradiation (or the equivalent time) the sample was kept under vacuum to avoid any contamination by air re-entering the sample.

3. Results and discussion

3.1 Absorption

We confirmed that addition of tubulin to TSPP results in a ~7 nm red shift associated with hypochromicity of the peak of the porphryin (Figure 1A) [25]. This is consistent with non-covalent complexation between the dye and the protein through electrostatic interactions between one or more of the four negatively charged SO_3^- groups in TSPP and positively charged residues in the tubulin dimer [25] with the addition of the possible rotation of the phenyl rings in-plane with the porphyrins macrocycle. Conversely, the absorption of tubulin does not appear to change upon binding of TSPP. The spectral differences shown in Figure 1B are the result of the overlapping absorption of TSPP in this region of the spectrum.

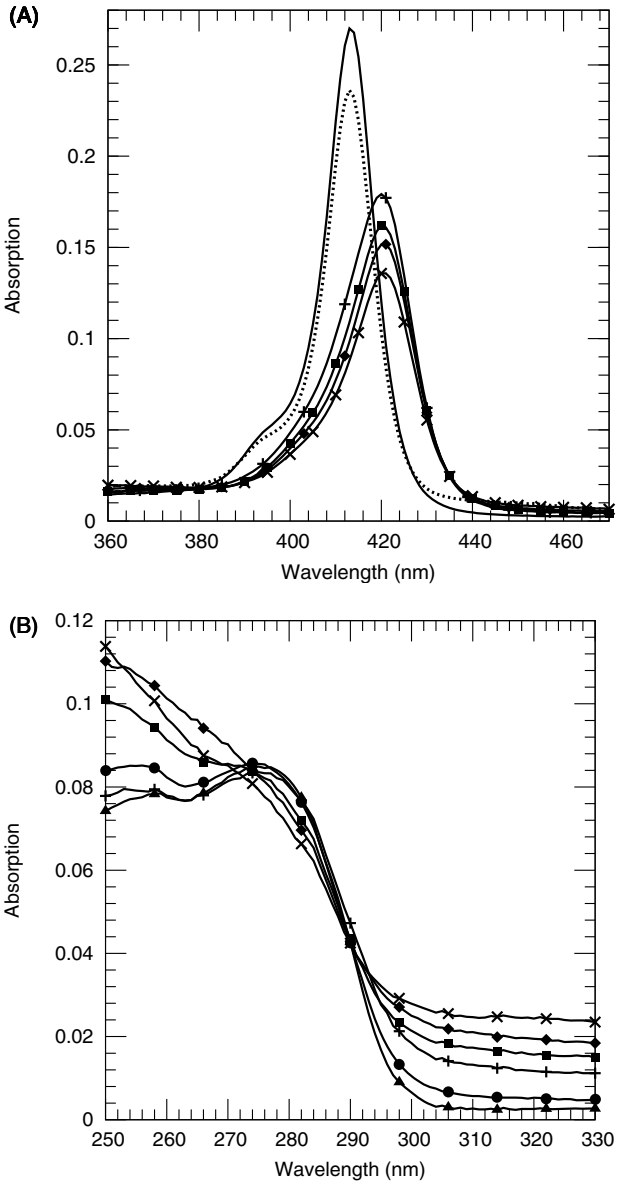

Figure 1 (**A**) Absorption spectra in the TSPP region with TSPP alone (solid line), TSPP irradiated 13.5 J/cm^2 (dashed line), tubulin/TSPP non-irradiated (++), tubulin/TSPP irradiated 4.5 J/cm^2 (squares), tubulin/TSPP irradiated 9 J/cm^2 (diamonds), tubulin/TSPP irradiated 13.5 J/cm^2 (××). (**B**) Absorption spectra for tubulin region with tubulin alone (triangles), tubulin irradiated 13.5 J/cm^2 (circles), tubulin/TSPP non-irradiated (++), tubulin/TSPP irradiated 4.5 J/cm^2 (squares), tubulin/TSPP irradiated 9 J/cm^2 (diamonds), and tubulin/TSPP irradiated 13.5 J/cm^2 (××).

Irradiating the TSPP/tubulin complex at 405 nm results in a 24% bleaching of the porphyrin absorption (Figure 1A) in agreement with the results obtained in a previous model [7, 8]. In this case, however, we do not observe a further red-shift of the Soret band of the porphyrin as a function of irradiation [7, 8]. The control carried out by irradiation of TSPP alone in aqueous solution does not lead to a shift in the absorption peak and only causes a 13% bleaching.

At the same time, irradiation of the TSPP/tubulin complex, changes the spectrum in the region of the aromatic amino acids of the protein. A shoulder appears around 300 nm which increases with irradiation of TSPP (Figure 1B). This spectral behavior was observed in a previous model and was attributed to the modification of a Trp residue [7, 8]. Since each tubulin monomer contains 4 Trp residues (in both the α and the β-variant) [45, 46], the results indicate that one or more of these residues are modified but our current data is unable to locate which residues undergo the modifications and further studies are being carried out to clarify this aspect. Irradiation of solutions containing tubulin alone does not affect the absorption spectrum of the protein.

3.2 Fluorescence

Addition of tubulin to TSPP in solution produces a red-shift of the fluorescence maximum (~5 nm) and a narrowing of the emission spectrum of TSPP (Figure 2A) which confirms the binding mechanism explained above.

Irradiation of TSPP in solution in the absence of tubulin shows a fluorescence photobleaching that parallels the decrease in absorption for the same sample (Figure 2A). Conversely, irradiation of the TSPP/tubulin complex produces a drastic (85%) decrease of the intrinsic fluorescence of tubulin (Figure 2B). Since tubulin does not absorb at 405 nm (the irradiation wavelength) the effect is explained as a photoinduced reaction between TSPP and the protein. Since tubulin fluorescence (at $\lambda_{ex} = 295$ nm) is exclusively produced by Trp residues, the decrease of the intrinsic tubulin fluorescence indicates an effect on one or more of these residues. These effects could include conformational and/or chemical changes of tubulin which are prompted by the irradiation of TSPP.

3.3 Fluorescence lifetime

To better understand the effects of TSPP irradiation on the protein we have recorded changes of the intrinsic fluorescence lifetime of tubulin. The fluorescence decay of the protein (Figure 3A) is best fitted by three exponential components which, because of the large number of Trp residues, are likely average values that encompass the non-exponential decays of each residue. The lifetimes can be summarized by a

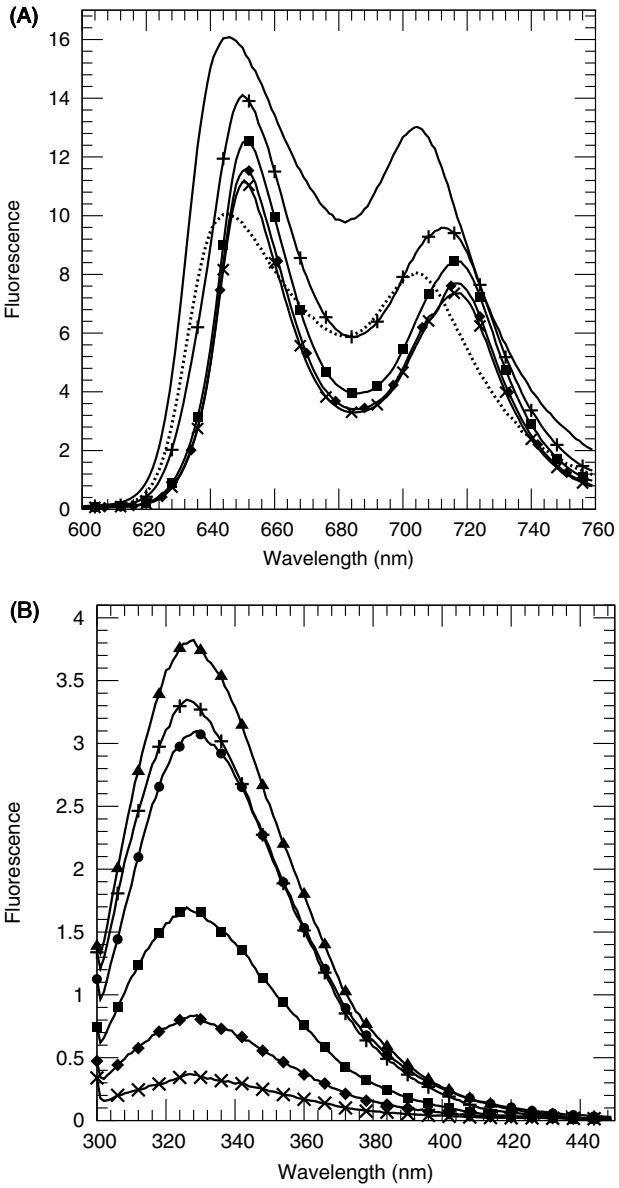

Figure 2 (**A**) Fluorescence spectra in TSPP region with TSPP alone (solid line), tubulin/TSPP complex non-irradiated (++), tubulin/TSPP complex irradiated 4.5 J/cm^2 (squares), tubulin/TSPP complex irradiated 9 J/cm^2 (diamonds), tubulin/TSPP complex irradiated 13.5 J/cm^2 (××), and TSPP irradiated 13.5 J/cm^2 (dashed line). (B) Fluorescence spectra for tubulin with tubulin alone (triangles), TSPP/tubulin non-irradiated (++), tubulin/TSPP complex irradiated 4.5 J/cm^2 (squares), tubulin/TSPP complex irradiated 9 J/cm^2 (diamonds), tubulin/TSPP complex irradiated 13.5 J/cm^2 (××), and tubulin irradiated 13.5 J/cm^2 (circles).

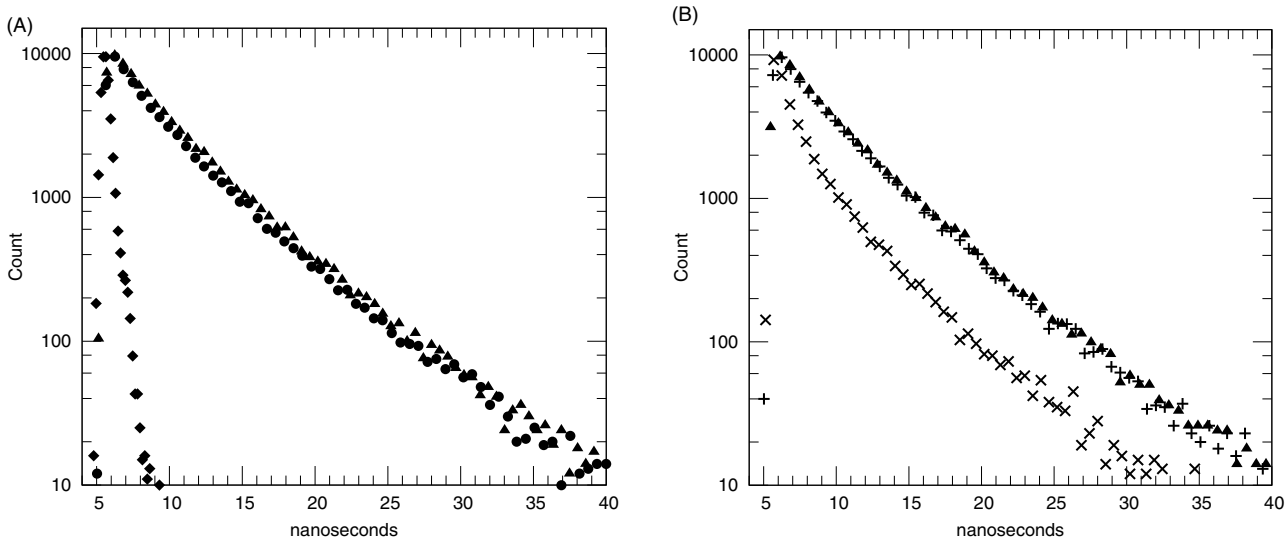

Figure 3 Fluorescence decay plots collected at 330 nm with an excitation source at 295 nm. (**A**) Tubulin (++) versus Tubulin Irradiated (triangles) and prompt scattering (circles). (**B**) Tubulin/TSPP complex (circles) versus Tubulin (++) and Tubulin/TSPP complex after irradiation with 13.5 J/cm^2 (triangles). The non-exponential fitting of each decay is shown as a solid line. The plot representative of the residuals is shown in the insert.

sub-nanosecond component with a small relative contribution (∼5%), an intermediate component of ∼3 ns with a relative contribution of ∼45% and a longer decay of ∼5.7 ns which contributes to ∼50% of the fluorescence signal (Table 1).

Binding of TSPP does not substantially affect the individual decay components (Figure 3A). The only effect is a small decrease of the relative contribution of the longer lived decay associated with a relative increase of the contribution of the intermediate component (Table 1). This enables us to rule out any significant energy transfer between the Trp residues and the porphyrin which is consistent with what was observed in a previous model [47].

Conversely, irradiation of the TSPP in the porphyrin/tubulin complex at 405 nm has a dramatic effect on the fluorescence decay of the protein (Figure 3B). The average lifetime Eq. (3) decreases from 4.12 ns to 2.41 ns at the end of the irradiation dose (Figure 3B). When considering the individual decay components (Table 1) one finds that the effect is both on the decay lifetime and the relative contribution. The shortest lifetime, τ_1, is at the limit of the temporal resolution of the system thus its fluctuation cannot be interpreted accurately. However, one observes an increase in its relative contribution. This might be significant but it does also include a relative increase of the scattering component due to the overall emission quenching (Figure 2B). Conversely, very significant are the sharp decreases in the intermediate (3.01 ns → 1.51 ns) and longer-lived (5.77 ns → 4.88 ns) components (Table 1). The intermediate lifetime is affected by a larger relative amount ($\Delta\tau \sim 1.5$ ns or 50% of the initial value) than the longer-lived component ($\Delta\tau \sim 0.9$ ns or 15% of the initial value). At the same time there is a sharp de-

Table 1 Fluorescence Lifetime Parameters of the Protein in the Irradiated Tubulin/TSPP Complex ($\lambda_{ex} = 295$ nm, $\lambda_{em} = 330$ nm ± 4 nm).

	Tubulin	Tubulin/TSPP 0 J/cm^2	Tubulin/TSPP 4.5 J/cm^2	Tubulin/TSPP 13.5 J/cm^2	Tubulin/TSPP 27 J/cm^2	Tubulin 13.5 J/cm^2
α_1	0.05 ± 0.01	0.06 ± 0.01	0.08 ± 0.01	0.14 ± 0.02	0.25 ± 0.02	0.08 ± 0.01
τ_1	0.34 ± 0.03	0.41 ± 0.02	0.26 ± 0.01	0.14 ± 0.01	0.14 ± 0.01	0.44 ± 0.02
α_2	0.43 ± 0.03	0.46 ± 0.03	0.36 ± 0.03	0.34 ± 0.03	0.38 ± 0.03	0.45 ± 0.03
τ_2	2.81 ± 0.09	3.01 ± 0.09	2.27 ± 0.07	1.69 ± 0.05	1.51 ± 0.04	2.67 ± 0.07
α_3	0.52 ± 0.01	0.47 ± 0.01	0.56 ± 0.01	0.52 ± 0.01	0.37 ± 0.01	0.48 ± 0.01
τ_3	5.68 ± 0.01	5.77 ± 0.03	5.24 ± 0.02	4.87 ± 0.02	4.88 ± 0.03	5.81 ± 0.02
$\langle\tau\rangle$	4.18	4.12	3.77	3.13	2.41	4.03

Time is given in nanoseconds and amplitudes are relative amplitudes.

crease in the relative contribution of both components, albeit difficult to interpret quantitatively because of the accompanying increase in the contribution of the sub-nanosecond component which as mentioned earlier approaches the limit of the temporal resolution. This effect is consistent with the decrease of fluorescence intensity shown in Figure 2B. To the best of our knowledge, the individual contribution of the 4 Trp residues to the fluorescence decay of tubulin has not been resolved; nevertheless the combined effects on steady-state emission and fluorescence decay indicate changes in the tertiary (and possibly secondary) structure of tubulin. It was shown that a similar effect is produced by the addition of guanidine hydrochloride and it was attributed to a dissociation of the α and β dimer followed by a partial unfolding of the monomers [48]. In view of the inhibition to the formation of MT (see below) the model presented by Sanchez et al. [48] might explain also the effects induced by the irradiation of TSPP. Nevertheless, at the moment we cannot rule out possible chemical modifications of the Trp residues as products of the irradiation [49]. Control experiments carried out by irradiating tubulin alone at 405 nm with the same light dose (13.5 J/cm^2 result in no significant change of fluorescence lifetime (Figure 3A) which indicates that the shortening of lifetime must be induced by the irradiation of the bound porphyrin.

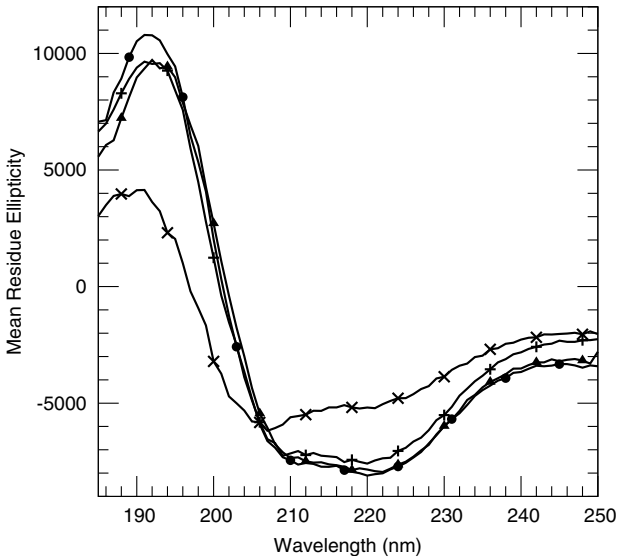

Figure 4 Circular Dichroism spectra of Tubulin alone ($\times\times$), Tubulin-TSPP complex (dotted line), Tubulin after irradiation 13.5 J/cm^2 (solid line), and Tubulin/TSPP complex after irradiation 13.5 J/cm^2 ($++$).

3.4 Circular dichroism

Binding of TSPP does not cause a significant change in the dichroic signal of tubulin and neither does the irradiation of the protein in the absence of TSPP (Figure 4, Table 2). Conversely, irradiation of the TSPP/tubulin complex produces a dramatic change in the CD spectrum. The double trough at 220 and 208 nm is drastically reduced while a negative peak at 206 nm becomes predominant. Also, the peak at 198 nm shifts by ~4 nm to shorter wavelengths. The negative peaks at 220 nm and 208 nm are typical of a α-helical structure. The analysis of the spectra with CDPro reveals that irradiation of the TSPP/tubulin complexes produces a 34% decrease in helical structure associated with a ~20% increase in the contribution of β-sheet and turns and an 11% increase in unordered structure. CDPro analysis is not always precise in terms of absolute numerical values [50], however it is valuable for qualitative information and reveals that changes occur in the secondary structure of tubulin with a substantial loss of helical contribution (Table 2). If one combines the information from CD spectroscopy with the changes in Trp fluorescence, a scenario emerges whereby irradiation of the porphyrin in the TSPP/tubulin complex prompts significant conformational changes in the protein.

TSPP alone did not show significant CD activity either in the UV or in the region of the Soret band (320 to 450 nm) before or after irradiation.

3.5 Atomic force microscopy

The significant effects on the secondary structure of tubulin prompted us to investigate how the irradiation of TSPP affects the formation of MTs *in vitro*. It can be seen from the images in Figure 5 that MT

Table 2 Secondary Structure composition of Tubulin, Tubulin/TSPP and Tubulin/TSPP irradiated at 413 nm using three fitting procedures.

	H(r)	H(d)	S(r)	S(d)	Trn	Und
Tubulin	0.148	0.124	0.151	0.097	0.210	0.268
Tubulin Irrad.	0.174	0.125	0.138	0.100	0.197	0.266
Tubulin/TSPP	0.148	0.124	0.151	0.096	0.212	0.270
Tubulin/TSPP Irrad.	0.081	0.099	0.186	0.112	0.224	0.299

formation is not significantly affected by binding of TSPP. Conversely, irradiation at 405 nm of the TSPP/tubulin complex results in the inhibition of MTs which is evident from the lack of fibrils and the presence of aggregated protein structures. This is most likely the result of the partial tubulin unfolding, revealed by fluorescence and CD experiments, which adversely affects the ability of tubulin to self-assemble into MT. The profile of Figure 5A shows that self-assembled MT formed before irradiation of the complex have a height of ∼10 nm and a diameter of ∼30 nm which is expected for MT which collapse when dried in air [51]. Self-assembly carried out with irradiated TSPP/tubulin complexes shows (Figure 5B) that MT are inhibited and replaced by globular aggregates with diameters of 80–100 nm.

3.6 *Deoxygenated samples*

Many porphyrins are known to populate their triplet state when optically excited. This has been the paradigm for their use in PDT where the porphyrin tri-

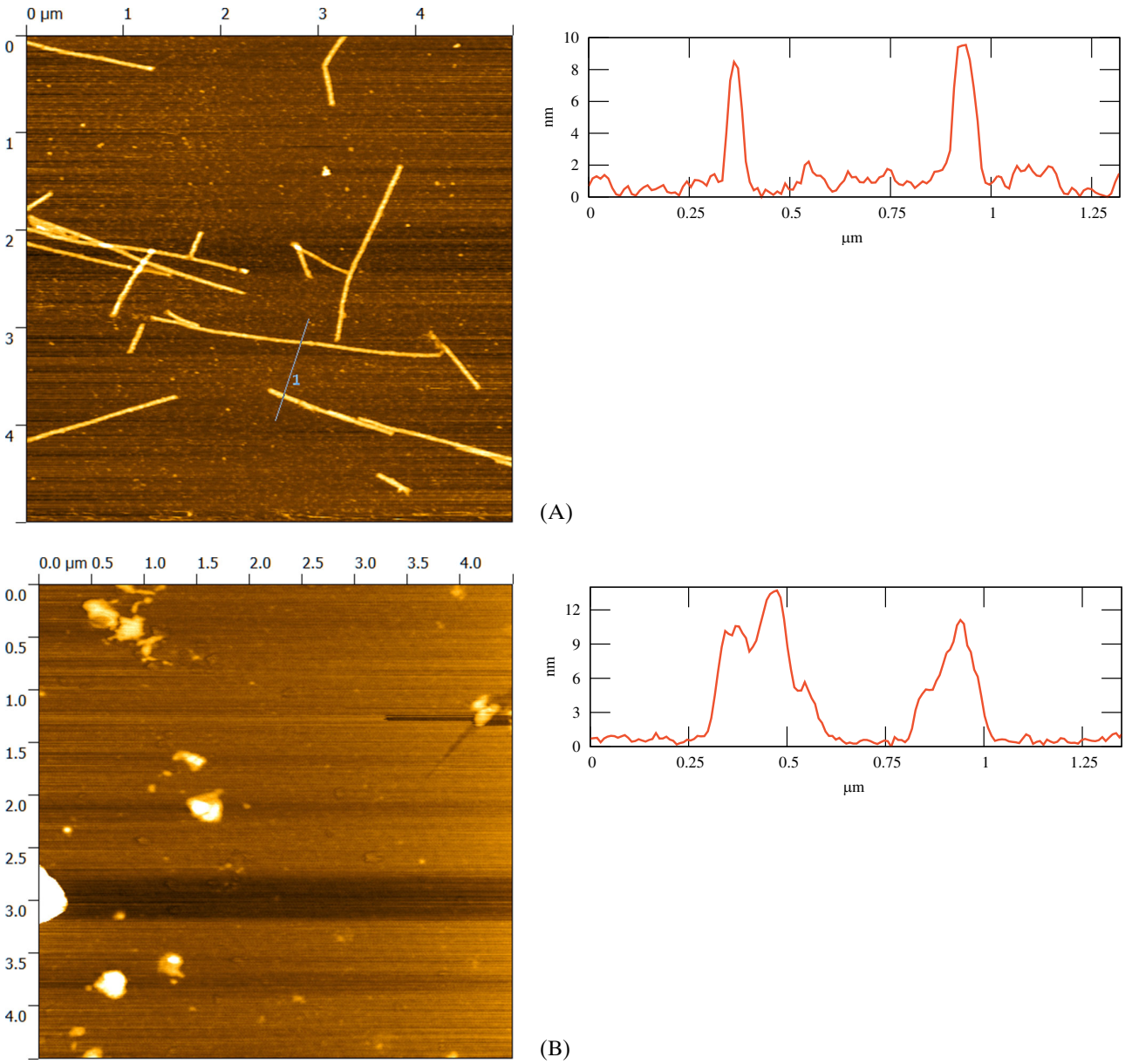

Figure 5 Atomic Force Microscopy images of (**A**) microtubules formed from tubulin in the presence of TSPP but not irradiated and (**B**) result of tubulin in the presence of TSPP when irradiated with 13.5 J/cm^2 at 413 nm and incubated in an assembly buffer.

plet state sensitizes the formation of singlet oxygen from diffusing O_2 [24]. This is a very probable mechanism since the triplet quantum yield of TSPP is 0.78 [52]. It is, therefore, important to establish whether the photoinduced effects on the protein structure are due to the sensitization of diffusing O_2 that prompts chemical modifications of tubulin, or if other photophysical/photochemical mechanisms are responsible for the effects. Thus, all the experiments described before were repeated (under the same conditions of irradiance and total energy) in samples deoxygenated through 5 cycles of freeze/thawing.

Freeze-thawing of the complex produces a further 1 nm red-shift (420 nm → 421 nm) of TSPP absorption maximum (Figure 6A) compared to the air-samples. This indicates that the porphyrin is still bound to tubulin after the deoxygenation procedure. Irradiation of the deoxygenated complex produces a negligible bleaching of TSPP (Figure 6A). On the other hand, bleaching of the tubulin still occurs (Figure 6B), albeit at a lesser rate than in air (Figure 1B). One also observes (Figure 6B) that the complex (as well as the control sample with tubulin alone) even before irradiation show a broad shoulder overlapped to the aromatic absorption of the protein. This is consistent with the presence of tubulin aggregates (not MT) [53], likely induced by the freeze-thaw cycles.

The fluorescence spectra of TSPP in the complex show that upon irradiation in a deoxygenated environment the porphyrin undergoes a very small (∼0.3%) bleaching (Figure 7B) compared to ∼18% in air (Figure 2A). Interestingly the steady state fluorescence of non-complexed tubulin (Figure 7B) shifts by ∼3 nm upon freeze-thawing without any significant loss of intensity. Conversely, freeze-thaw of the complex produces a substantial decrease of the emission of the protein but no red-shift of the emission. This indicates that tubulin is susceptible to the freeze-thaw deoxygenation method but that binding of TSPP stabilizes the protein and prevents possible changes of tertiary structure shown by tubulin alone (i.e., the red-shift of the emission maximum). Despite the negligible bleaching of TSPP upon irradiation (Figure 7A), which would suggest a lack of photoreactivity in the absence of O_2, the Trp fluorescence of tubulin is drastically reduced to an extent similar (75% vs. 90% decrease) to what occurs in air samples (Figure 2B). Therefore the steady-state fluorescence data indicate that, despite the absence of porphyrin photobleaching, photoinduced mechanism are still occurring and affecting the environment of Trp residues even in deoxygenated TSPP/tubulin complexes. What appears to be hindered is the presence of further chemical steps (as seen by the lack of the 300 nm shoulder in Figure 6B).

As mentioned earlier, deoxygenation with the freeze/thaw process appears to lead to aggregation of tubulin prior to irradiation. This structural change is confirmed by fluorescence lifetime which decreases slightly (∼0.3 ns as shown in Table 3) upon this freeze/thaw process. However, irradiation of the deoxyge-

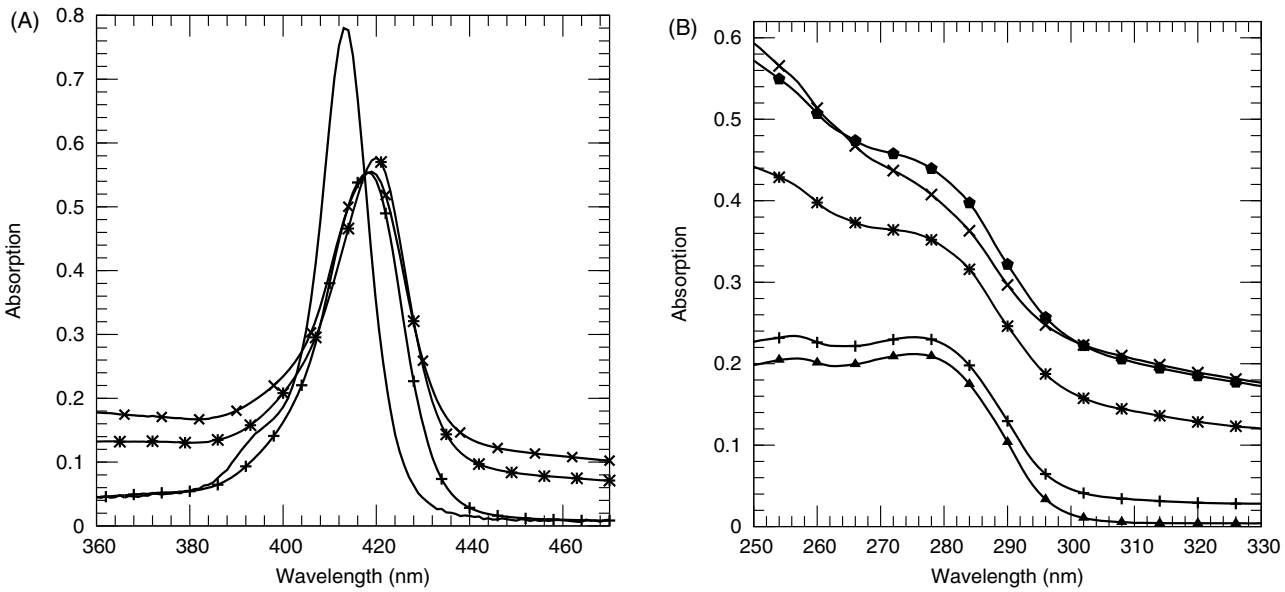

Figure 6 Absorption spectra for samples deoxygenated via freeze/thaw process. (**A**) Absorption spectra in the TSPP region with TSPP alone (××), Tubulin/TSPP complex (solid line), Tubulin/TSPP complex deoxygenated (triangles), Tubulin/TSPP complex deoxygenated and irradiated 13.5 J/cm^2 (dotted line). (**B**) Absorption spectra in the tubulin region with Tubulin alone (++), Tubulin deoxygenated (××), Tubulin/TSPP complex (triangles), Tubulin/TSPP complex deoxygenated (dotted line) and Tubulin/TSPP complex deoxygenated and irradiated 13.5 J/cm^2 (solid line).

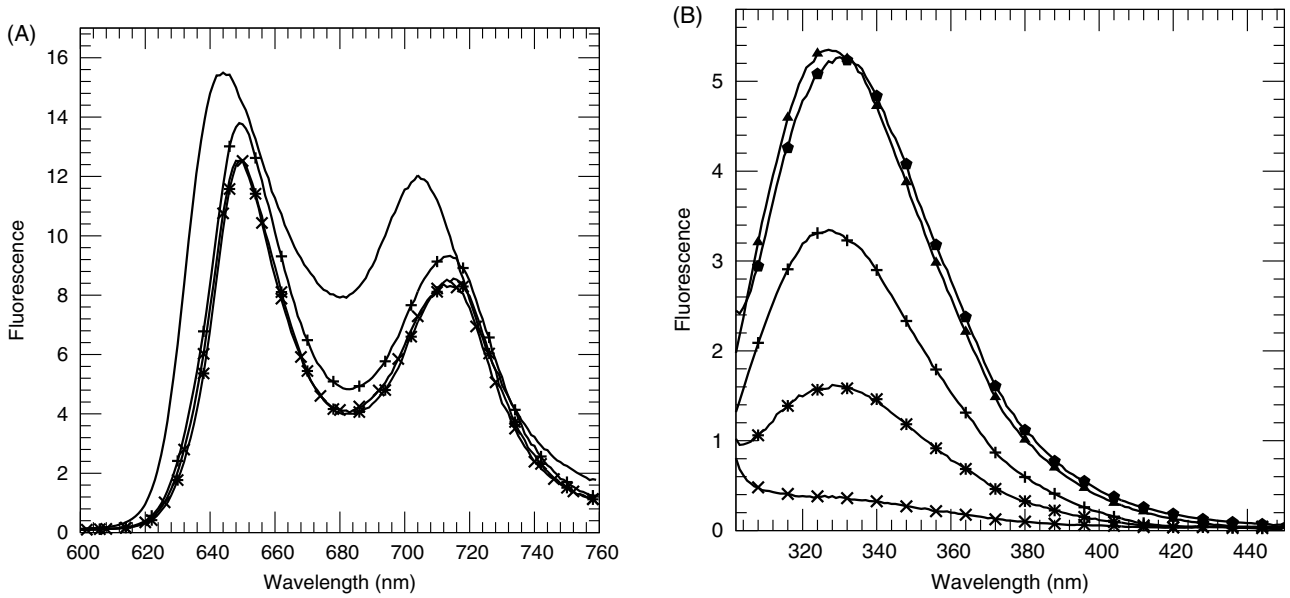

Figure 7 Fluorescence spectra for samples deoxygenated via freeze/thaw process. (**A**) Fluorescence spectra for TSPP with TSPP alone (solid line), Tubulin/TSPP complex (triangles), Tubulin/TSPP complex deoxygenated (dotted line) and Tubulin/TSPP deoxygenated and irradiated 13.5 J/cm^2 ($\times\times$). (**B**) Fluorescence spectra for Tubulin with Tubulin alone (solid line), Tubulin/TSPP complex (dotted line), Tubulin alone deoxygenated (triangles), Tubulin/TSPP complex deoxygenated ($\times\times$) and Tubulin/TSPP complex deoxygenated and irradiated 13.5 J/cm^2 (circles).

nated tubulin/TSPP complex at 413 nm produces an additional decrease in average lifetime of the protein (from 2.14 ns to 1.05 ns) as shown by Figure 8. This implies that conformational changes affecting the environment surrounding one or more Trp residues still occur in tubulin despite removal of O_2. The data suggest that although freeze-thaw prompts the aggregation of some of the tubulin in solution, the tubulin that is left and forms the complex with TSPP still undergoes structural changes upon irradiation. Therefore we believe that the initial photophysical trigger of the conformational modifications is not photosensitized singlet oxygen but some other direct mechanism such as, for instance, charge transfer and that O_2 is involved only in subsequent mechanism responsible for the appearance of the shoulder at 320 nm (Figure 1B) and the larger bleaching of TSPP (Figure 1A and 2A).

Considering the steady-state and lifetime data in air and in deoxygenated sample (Figure 2B, Figure 3, Figure 7B and Figure 8) it is clear that the Trp fluorescence of the protein is affected by the irradiation of the complex and that such change produces similar effects with or without O_2. Such evidence is consistent with conformational changes that may move quenching groups (His, amides, Cys) close to one or more Trp residues or the partial exposure and/or increased mobility of one or more Trp residues.

Table 3 Fluorescence Lifetime Parameters of the Protein in the Irradiated Tubulin/TSPP Complex ($\lambda_{ex} = 295$ nm, $\lambda_{em} = 330$ nm $\pm$ 4 nm) for experiment of samples deoxygenated with freeze/thaw process.

	Tubulin	Tubulin/TSPP	Tubulin Deoxy	Tubulin/TSPP Deoxy	Tubulin/TSPP Deoxy + 13.5 J/cm^2
α_1	0.04 $\pm$ 0.01	0.06 $\pm$ 0.01	0.07 $\pm$ 0.01	0.20 $\pm$ 0.03	0.43 $\pm$ 0.02
τ_1	0.51 $\pm$ 0.05	0.28 $\pm$ 0.01	0.37 $\pm$ 0.01	0.30 $\pm$ 0.06	0.07 $\pm$ 0.01
α_2	0.43 $\pm$ 0.02	0.36 $\pm$ 0.02	0.46 $\pm$ 0.03	0.50 $\pm$ 0.02	0.38 $\pm$ 0.03
τ_2	2.92 $\pm$ 0.05	2.55 $\pm$ 0.06	2.53 $\pm$ 0.04	1.60 $\pm$ 0.03	0.99 $\pm$ 0.02
α_3	0.53 $\pm$ 0.01	0.58 $\pm$ 0.01	0.47 $\pm$ 0.03	0.30 $\pm$ 0.02	0.19 $\pm$ 0.02
τ_3	5.74 $\pm$ 0.02	5.40 $\pm$ 0.03	6.00 $\pm$ 0.02	4.28 $\pm$ 0.02	3.37 $\pm$ 0.03
$\langle\tau\rangle$	4.31	4.07	4.01	2.14	1.05

Time is given in nanoseconds and amplitudes are relative amplitudes.

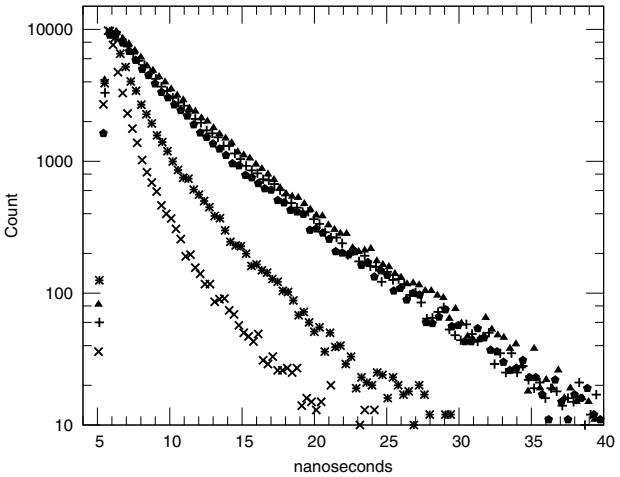

Figure 8 Fluorescence decay plot collected at 330 nm with an excitation source at 295 nm for experiment deoxygenated with freeze/thaw process. Tubulin in normal oxygen environment (triangles), Tubulin alone deoxygenated (++), Tubulin/TSPP complex (circles), Tubulin/TSPP complex deoxygenated (××), and Tubulin/TSPP complex deoxygenated and irradiated with 13.5 J/cm^2 (diamonds). The non-exponential fitting of each decay is shown as a solid line. The plot representative of the residuals is shown in the insert.

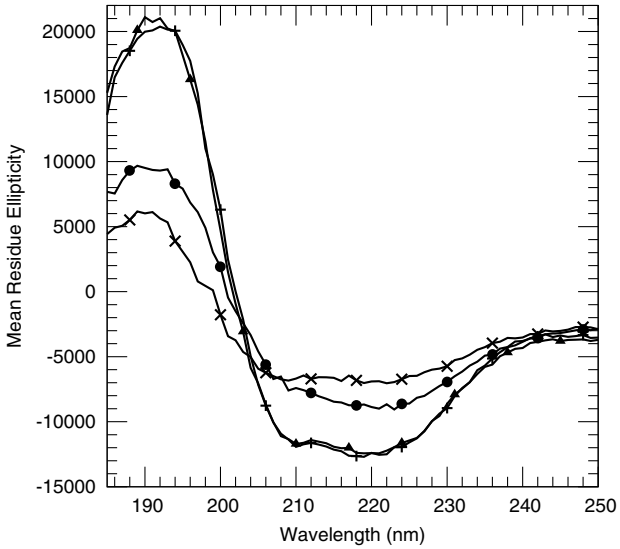

Figure 9 Circular Dichroism spectra for freeze/thaw deoxygenation experiment. Tubulin alone (××), Tubulin-TSPP complex (dotted line), Tubulin deoxygenated and irradiated with 13.5 J/cm^2 (solid line), and Tubulin/TSPP complex deoxygenated and irradiated 13.5 J/cm^2 (++).

Comparison of Tables 3 and 4 as well as the CD spectra of Figures 4 and 9 shows that freeze-thaw does not induce major changes in the secondary structure of tubulin. This validates our interpretation that the changes in tubulin fluorescence produced by freeze-thaw are due to aggregation. The sharp decrease in overall CD intensity after irradiation of tubulin alone is not entirely clear but could be explained with some degree of aggregation of the protein, however the comparison among the single secondary structure components reveals only minor secondary conformational changes compared to the corresponding sample in air-saturated solutions of Table 2 (a small increase in helical and unordered component and a small decrease in β-sheet and turns contribution). In agreement with the fluorescence and fluorescence lifetime data, irradiation of the complex under deoxygenated conditions is still capable of producing changes in the secondary structure of tubulin (Figure 9 and Table 4) despite the substantial lack of TSPP photobleaching (Figure 7). The photoinduced changes are highlighted by a 22% decrease in helical component accompanied by a simultaneous increase of β-sheet and turns contribution (19%) as well as unordered structure (3%).

AFM was also performed on a solution of tubulin that underwent the freeze-thaw cycle. Unfortunately, (Figure 10) aggregates appear to dominate the scans, but it validates our hypothesis regarding the formation of aggregates of otherwise intact tubulin. These aggregates have larger diameters (>100 nm) than the one produced by irradiation in air-saturated samples (Figure 5B).

Table 4 Secondary Structure composition of Tubulin, Tubulin/TSPP complex, Tubulin/TSPP complex deoxygenated, and Tubulin/TSPP complex irradiated and deoxygenated. Irradiation performed at 413 nm with dosage 13.5 J/cm^2 and samples deoxygenated with freeze/thaw procedure.

	H(r)	H(d)	S(r)	S(d)	Trn	Und
Tubulin	0.247	0.156	0.066	0.059	0.199	0.273
Tubulin/TSPP	0.251	0.148	0.080	0.060	0.189	0.272
Tubulin/TSPP Deoxy.	0.160	0.130	0.133	0.085	0.208	0.284
Tubulin/TSPP Deoxy. Irrad.	0.117	0.109	0.162	0.102	0.218	0.293

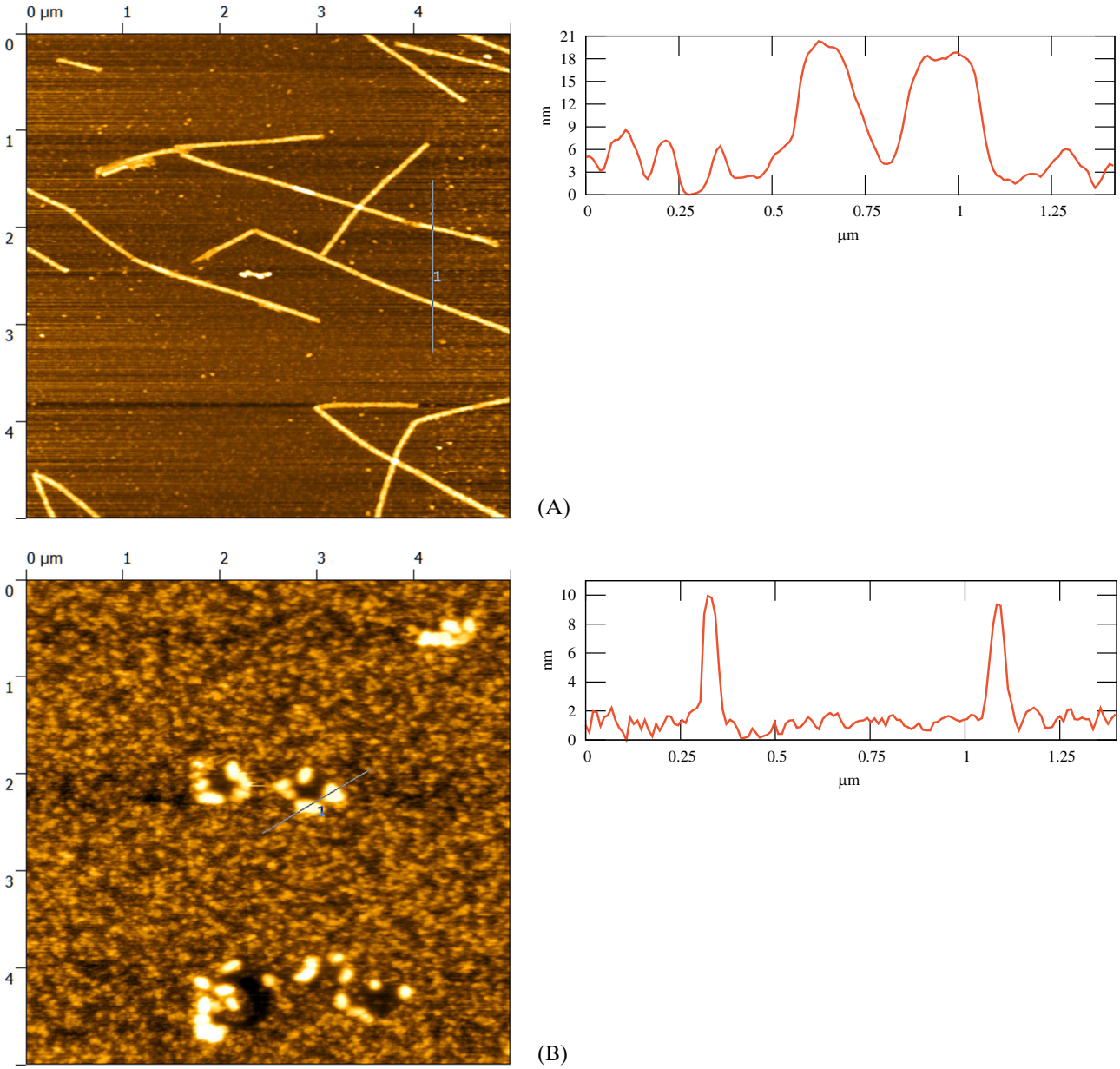

Figure 10 Atomic Force Microscopy images of (**A**) solution of tubulin subjected to the freeze-thaw cycle and incubated in assembly buffer resulting in aggregates (**B**) microtubules formed from a solution of tubulin alone after being irradiated with 13.5 J/cm^2 at 413 nm and incubated in assembly buffer.

4. Conclusions

The overall results indicate clear evidence for the partial unfolding of tubulin triggered by the optical excitation of TSPP in the protein/porphyrin non-covalent complex. Compared to previous results on a different protein model [7, 8], irradiation of the TSPP/protein complex does not prompt a rearrangement of the porphyrin conformation. Our data show that neither TSPP alone or laser irradiation alone are capable of producing detectable conformational changes in tubulin, therefore the structural modifications are entirely mediated by the photophysical and photochemical interactions between the excited state of TSPP and the protein (likely in proximity of the binding site). The use of low irradiance (<20 mW/cm^2) and low dye concentration (<1 µM) enables us to rule out thermal effects due to laser irradiation [43], thus, we conclude that the partial unfolding effects are photochemical/photophysical in nature.

RRS (Figure S5 and Table S3 in Supporting Information) and fluorescence shows that the structure

of TSPP does not change upon irradiation and that no fluorescent photoproducts are produced, suggesting that photoinduced effects are not due to permanent changes in the ligand (e.g., porphyrin photoproducts) and are instead due to mechanisms triggered by the irradiation of the ligand but occurring at the level of the protein backbone or of the amino acid residues.

The intrinsic fluorescence and fluorescence lifetime of tubulin as well as the CD spectra provide the most convincing evidence of conformational changes in tubulin which included both the secondary and tertiary structure. Irradiation of the complex produces a decrease of the helical component and a simultaneous increase of β-structures (sheets and turns) and unordered chains. The exact location of these changes is still unknown and is the focus of our ongoing investigation. The mechanism responsible for triggering the conformational effects is also still under investigation as we so far lack direct evidence, however based on the results described here there seems to be a dual action initiated by TSPP. This porphyrin has been studied as a potential phototherapeutic drug [54] and has a large quantum yield of intersystem crossing to a triplet state [55]. Therefore, it was tempting to explain the photoinduced effects on the protein as a result of photosensitization of singlet oxygen followed by reactions with the backbone or the side chains of the amino acids in tubulin. However, the removal of oxygen from the solution does not prevent the partial unfolding of tubulin. Thus, sample deoxygenation suppresses the photobleaching of TSPP and reduces but does not eliminate its ability to induce partial unfolding of the tubulin. Therefore, O_2-independent mechanisms are still able to prompt the conformational changes. As mentioned earlier at the moment we believe that the initial mechanism that triggers the conformational changes could be interpreted as a direct charge transfer from TSPP to the protein [55]. In deoxygenated samples this mechanism is the only event and prompts some rearrangement in the protein structure (as shown by the spectroscopic data). In the presence of O_2 (air-saturated samples) the initial event is followed by reaction with oxygen and leads to both further structural changes in the protein but also chemical modifications not detected in the absence of oxygen (i.e., TSPP photobleaching, 320 nm absorption shoulder in the protein spectrum) that could drive additional conformational changes in the protein.

Finally our results show that the TSPP-photoinduced conformational changes are able to inhibit the formation of MT *in vitro*. This indicates that tubulin has been modified to the extent that prevents the growth of fibrils in the direction of the long axis of the MT. Although identifying the location of the photoinduced changes requires additional (ongoing) investigations, we have demonstrated that porphyrins are promising mediators of direct protein inactivation through visible irradiation. This finding could open the possibility of changing the strategic utilization of these compounds in biomedical applications.

Acknowledgements The research was in part funded by a seedling grant from the Air Force Research Laboratory (FA8650-07-D-6800) to R.J.T. and a TASC subcontract ORESS FA8650-08-D-6930 to L.B. B.M. is supported by the Consortium Research Fellows Program (FA8650-13-2-6366). The authors would also like to thank Jim Parker and Gary Noojin for their technical support.

Author biographies Please see Supporting Information online.

References

[1] K. E. van Holde, W. C. Johnson, and P. S. Ho, Principles of Physoical Biochemistry (Pearson Prentice Hall, Upper Saddle River, NJ, 2006).
[2] V. Muñoz, Annu Rev Biophys Biomol Struct. **36**, 395–412 (2007).
[3] C. T. Lee Jr, K. A. Smith, and T. A. Hatton, Biochemistry **44**, 524–536 (2005).
[4] M. Loweneck, A. G. Milbradt, C. Root, H. Satzger, W. Zinth, L. Moroder, and C. Renner, Biophys. J. **90**, 2099–2108 (2006).
[5] K. Jacobson, Z. Rajfur, E. Vitriol, and K. Hahn, Trends Cell Biol., **18**, 443–450 (2008).
[6] D. G. Jay, Proc. Natl. Acad. Sci. **85**, 5454–5458 (1988).
[7] N. F. Fernandez, S. Sansone, A. Mazzini, and L. Brancaleon, J. Phys. Chem. B **112**, 7592–7600 (2008).
[8] N. F. Fernandez, S. Sansone, J. Belcher, W. E. Haskins, and L. Brancaleon, J. Phys. Chem. B **113**, 6020–6030 (2009).
[9] J. E. Parker, R. J. Thomas, D. Morisson, and L. Brancaleon, J. Phys. Chem. B **116**, 11032–11040 (2012).
[10] M. Caplow and L. Fee, Mol. Biol. Cell **13**, 2120–2131 (2002).
[11] E. Nogales and H. W. Wang, Curr Opin Cell Biol. **18**, 179–184 (2006).
[12] S. K. Dutcher, Curr Opin Cell Biol. **13**, 49–54 (2001).
[13] E. Nogales, K. H. Downing, L. A. Amos, and J. Löwe, Nat Struct Biol. **5**, 451–458 (1998).
[14] E. Nogales and H. W. Wang, Curr Opin Struct Biol. **16**, 221–229 (2006).
[15] K. H. Downing and E. Nogales, Curr. Op. Struct. Biol. **8**, 785–791 (1998).
[16] J. Zhou and P. Giannakakou, Curr. Med. Chem. Anticancer Agents **5**, 65–71 (2005).
[17] S. Honore, E. Pasquier, and D. Braguer, Cell. Mol. Life Sci. **62**, 3039–3056 (2005).
[18] E. Pasquier and M. Kavallaris, IUBMB Life **60**, 165–170 (2008).
[19] J. P. Snyder, J. H. Nettles, B. Cornett, K. H. Downing, and E. Nogales, Proc. Natl. Acad. Sci. **98**, 5312–5316 (2001).

[20] R. Bonnett and G. Martinez, Org. Lett. **4**, 2013–1016 (2002).
[21] A. P. Castano, P. Mroz, and M. R. Hamblin, Nat Rev. Canc. **6**, 535–545 (2006).
[22] M. Ethirajan, Y. Chen, P. Joshi, and R. K. Pandey, Chem Soc Rev. **40**, 340–362 (2011).
[23] B. C. Wilson and M. S. Patterson, Phys Med Biol. **53**, R61–R109 (2008).
[24] E. D. Sternberg, D. Dolphin, and C. Brickner, Tetrahedron **54**, 4151–4202 (1998).
[25] F. Tian, E. M. Johnson, M. Zamarripa, S. Sansone, and L. Brancaleon, Biomacromol. **8** 3767–3778 (2007).
[26] H. Guo, C. Xu, C. Liu, E. Qu, M. Yuan, Z. Li, and B. Cheng, Biophys J. **90**, 2093–2098 (2006).
[27] J. R. Lakowicz, Principles of Fluorescence Spectroscopy, 3rd ed. (Springer, New York, 2006).
[28] S. M. Andrade and S. M. B. Costa, Biophys. J. **82**, 1607–1619 (2002).
[29] N. K. Subbarao and R. C. MacDonald, Analyst **118**, 913–916 (1993).
[30] F. V. Bright and C. Munson, Anal. Chim. Acta **500**, 71–104 (2003).
[31] Z. Li, T. Lu, T. He, F. Liu, and D. Chen, Chinese J. Chem. Phys. **22**, 346–352 (2009).
[32] S. M. Kelly, T. J. Jess, and N. C. Price, Biochim Biophys Acta **1751**, 119–139 (2005).
[33] C. W. Johnson, Circular Dichroism and the Conformational Analysis of Biomolecules, Circular Dichroism and the Conformational Analysis of Biomolecules (1996), pp. 635–653.
[34] N. J. Greenfield, Nat. Protoc. **1**, 2876–2890 (2006).
[35] N. Sreerama and R. W. Woody, Anal Biochem. **287**, 252–260 (2000).
[36] J. Lowe, H. Li, K. H. Downing, and E. Nogales, J. Mol. Biol. **313**, 1045–1057 (2001).
[37] D. Hall and A. P. Minton, Anal. Biochem. **345**, 198–213 (2005).
[38] R. L. Margolis, Proc. Natl. Acad. Sci. **78**, 1586–1590 (1981).
[39] I. Arnal and R. H. Wade, Curr. Biol. **5**, 900–908 (1995).
[40] Y. L. Lyubchenko and L. S. Shlyakhtenko, Methods **47**, 206–213 (2009).
[41] D. J. Field, R. Collins, and J. C. Lee, Proceed. Nat. Acad. Sci. **81**, 4041–4045 (1984).
[42] R. C. Williams, C. Shah, and D. Sackett, Anal Biochem. **275**, 265–267 (1999).
[43] C. D. Clark, M. L. Denton, and R. J. Thomas, J. Biomed. Opt. **16**, 020504 (2011).
[44] F. Cioci and R. Lavecchia, Am. Inst. Chem. Engin. J. **43**, 525–534 (1997).
[45] E. Krauhs, M. Little, T. Kempf, and H. Ponstingl, Proc Natl Acad Sci USA **78**, 2757–2761 (1981).
[46] E. Krauhs, M. Little, T. Kempf, and H. Ponstingl, Proc Natl Acad Sci USA **78**, 4156–4160 (1981).
[47] F. Tian, K. Johnson, A. E. Lesar, H. Moseley, J. Ferguson, I. D. W. Samuel, A. Mazzini, and L. Brancaleon, Biochim. Biophys. Acta **1760**, 38–46 (2005).
[48] S. A. Sanchez, J. E. Brunet, D. M. Jameson, R. Lagos, and O. Monasterio, Protein Sci. **13**, 81–88 (2004).
[49] P. S. Sherin, O. A. Snytnikova, and Y. P. Tsentalovich, Chem. Phys. Lett. **391**, 44–49 (2004).
[50] N. Sreerama and R. W. Woody, Anal. Biochem. **209**, 32–44 (2003).
[51] L. Hamon, P. Curmi, and D. Pastre, Method. Cell Biol. **95**, 157–174 (2010).
[52] L. P. F. Aggarwal, M. S. Baptista, and I. E. Borissevitch, J. Photochem. Photobiol. A **186**, 187–193 (2007).
[53] V. Prakash and S. N. Timasheff, Arch Biochem Biophys. **295**, 137–145 (1992).
[54] A. P. Thomas, P. S. Saneesh Babu, S. Asha Nair, S. Ramakrishnan, D. Ramaiah, T. K., Chandrashekar, A. Srinivasan, and M. Radhakrishna Pillai, J Med Chem. **14**, 5110–5120 (2012).
[55] J. Mosinger, M. Deumie', K. Lang, P. Kubat, and D. M. Wagnerova, J. Photochem. Photobiol. A **130**, 13–20 (2000).